Eur. Phys. J. D **7**, 595–599 (1999)

THE EUROPEAN PHYSICAL JOURNAL D

EDP Sciences

Impact induced adsorption of C_{20} on silicon (001) surface

Z.Y. Man[1,2], Z.Y. Pan[1,2,a], Y.K. Ho[1,3], and W.J. Zhu[1,2]

[1] State Key Laboratory for Material Modification by laser, ion and electron beams, Institute of Modern Physics, Fudan University, Shanghai 200433, P.R. China
[2] Ion beam laboratory, Shanghai Institute of Metallurgy, Academia Sinica, Shanghai, P.R. China
[3] CCAST, World Laboratory, P.O. Box 8730, Beijing 100080, P.R. China

Received 12 March 1999 and Received in final form 20 May 1999

Abstract. Molecular dynamics simulations were carried out to investigate the adsorption of a low-energy C_{20} on a reconstructed silicon (001)-(2 × 1) surface. The impact energies of the C_{20} fullerene range from 1 eV/atom to 5 eV/atom. After impacting, the C_{20} molecule is found to move along (011) direction and resides either in the trough or on the dimer at the end of our simulations. The lateral motion of C_{20} on the surface is dependent on its incident energy. Chemical bonds are formed between C_{20} and the surface. By the force field analysis, we show that the anisotropic molecule-surface interaction plays the leading role in the lateral motion of C_{20} as well as its preferable adsorption sites on the dimerized Si surface. These findings are consistent with experimental observations of C_{60} on Si (001) surface and small carbon clusters on solid surfaces.

PACS. 79.20.Rf Atomic, molecular, and ion beam impact and interactions with surfaces – 36.40.Qv Stability and fragmentation of clusters – 61.46.+w Clusters, nanoparticles, and nanocrystalline materials

1 Introduction

Fullerene-surface interaction has attracted a great deal of interest due to its peculiarity as well as promising application in synthesis of nanostructured thin-films. In the past decade, most of research has been concentrated on the C_{60} and C_{70} molecules, both experimentally [1–3] and theoretically [4–7]. Much less is known about the interaction of small fullerenes with surfaces. Experimentally, neutral small carbon clusters ($C_{20} \sim C_{32}$) with low kinetic energy (∼10 eV) have been deposited on various substrates to produce thin-films of novel properties [8]. The most fascinating is the "C_{20}-type films", which is formed by deposition of clusters with distribution centered around C_{20}. It presents sp^3-hybridization strongly as the spectra in C_{20}, and a new disordered form of diamond-like films. C_{20} is theoretically expected to be the smallest possible cluster that can form a closed fullerene structure [9]. It has 12 pentagons and each carbon atom has a dangling bond (threefold bonded). It is known that both molecule-molecule and molecule-surface interaction play important roles in the growth process of thin-films. At atomic level understanding of the interaction between C_{20} and surface is highly desired.

In this paper, we focus our attention on the C_{20}–Si (001)-(2×1) surface interaction. The impact-induced adsorption of C_{20} is simulated. The collective motion of the C_{20} cluster and its preferable adsorption configuration on an anisotropic surface are investigated. The results are explained by surface force field analysis at atomic level. These interaction characteristics found in this study are known to play a crucial role to the microscopic diffusion of cluster and have close relationship with the long-range disorder of the film [10].

2 Simulation model

The interactions between carbon and silicon atoms are described by a hybrid potential, which combines the Tersoff potential [11] and the KrC potential [12]. Tersoff potential function has been proved to be a suitable one to describe the carbon and silicon system. With Tersoff potential, the bulk properties and the surface reconstruction of diamond [13], silicon [14] and SiC [15] were reproduced. We have also calculated the structure properties of C_{60} and C_{70} fullerenes [16] by using the Tersoff potential. For the C_{20} fullerene, the calculated average bond length and the cohesive energy are 1.53 Å and 116.3 eV (5.8 eV/atom), respectively. These data are in agreements with the *ab initio* calculations [17]. Unfortunately, in this potential the repulsive part at short internuclear separations is not strong

[a] *Mailing address*: Institute of Modern Physics, Fudan University, Shanghai 200433, P.R. China.
e-mail: hoyk@fudan.ac.cn

enough. Thus a screened Coulomb potential, *i.e.*, the KrC potential is used to describe the short distance interactions between C–C, C–Si and Si–Si [12,18,19]. The combined potential consists of KrC function splined to Tersoff potential smoothly by choosing reasonable connection points

$$\begin{cases} V(r < r_1) & = V_{\mathrm{KrC}}(r) \\ V(r_1 < r < r_2) & = V_{\mathrm{spline}}(r) \\ V(r > r_2) & = V_{\mathrm{Tersoff}}(r) \end{cases} \quad (1)$$

where r is the interatomic distance and r_1 and r_2 are the connection points. We choose three different sets of r_1 and r_2 to ensure smoothness and continuity of the potential and force for the C–C, C–Si and Si–Si interactions. The adopted values of the connection points are as follows: $r_1 = 0.35$ Å, $r_2 = 0.55$ Å for C–C interaction, $r_1 = 0.4$ Å, $r_2 = 0.6$ Å for C–Si interaction, and $r_1 = 0.45$ Å, $r_2 = 0.65$ Å for Si–Si interaction. It has also been checked that the splines do not change the calculated static properties of fullerenes, diamond, silicon and silicon carbide. Those results can be well understood because the static properties chiefly depend on the medium and long range parts of the potential.

The silicon substrate in our simulation model consists of 10 layers of atoms with 400 atoms per layer. Periodic boundary conditions are applied in the x and y orthogonal directions parallel to the (001) surface. The motion of the two top layers of silicon atoms as well as the C_{20} projectile atoms are derived directly from the Newtonian equations with the interaction potential described above. The temperature of the next six layers are kept constant by velocity rescaling method [20]. In practice, the rescaling coefficient has been held to be less than 0.1% in each time step. The bottom two layers are fixed so that no reconstruction occurs here. We first generate a (2×1) reconstructed silicon surface (001). Then the C_{20} cluster is initially placed above the surface at a distance where the interactions with the silicon substrate are negligible. Both the C_{20} and the silicon substrate are thermalized at 300 K before the collision starts. The C_{20} molecule is set to impact normally on the silicon substrate with incident energies from 1 eV/atom to 5 eV/atom. The equations of motion are integrated according to the "leap frog" form of the Verlet algorithm [21] with a variable time step ranging from 0.2 fs to 0.6 fs. In addition, the simulation model has been examined by increasing the number of top layers in the target without velocity rescaling from two to four and decreasing the number of frozen layers from six to four correspondingly. About the same results are observed when the collision conditions are the same.

3 Results and discussions

To gain some general features of the interaction process, ten impact events with impact positions randomly selected between point A and point C (see Fig. 1) have been simulated at the impact energy of 5 eV/atom. The orientation of C_{20} is randomly selected too. The results show that the

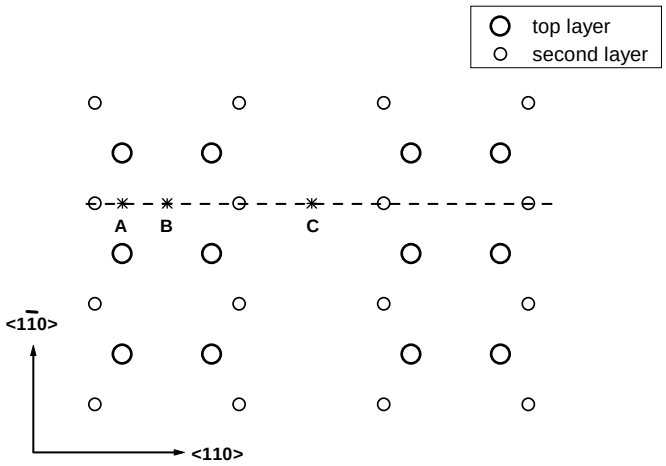

Fig. 1. Schematic of the impact positions (A, B and C) of the C_{20} molecules on the silicon (001)-(2×1) surface.

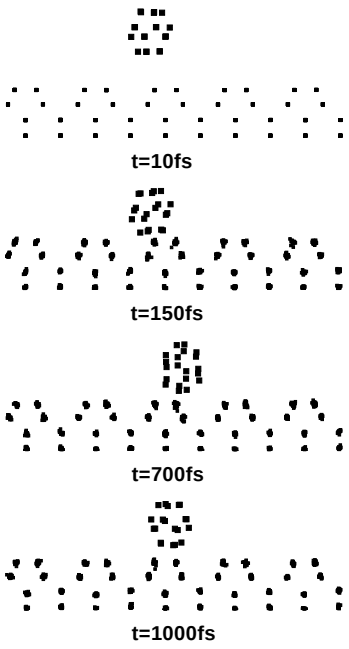

Fig. 2. Snapshots of the atomic positions of the C_{20} and the reconstructed Si (001) surfaces at different times during the collision. The impact energy of C_{20} cluster is 5 eV/atom.

C_{20} molecule moves either to the dimer or to the trough in the end. In the following discussions, we will focus on a single impact process to study the influence of the impact energy and impact points. The orientation of C_{20} is arranged in such a way that its atoms closed to the substrate form a pentagon parallel to the silicon surface ("pentagon down" configuration). The impact points on the dimerized surface are selected at A, B and C shown in Figure 1. Figure 2 shows a snapshots of a typical interaction processes (5 eV/atom). With a translational energy of 5 eV/atom the C_{20} cluster impacts at position A. After arriving on the silicon surface the C_{20} rolls as a sphere on it since the interaction are usually asymmetric.

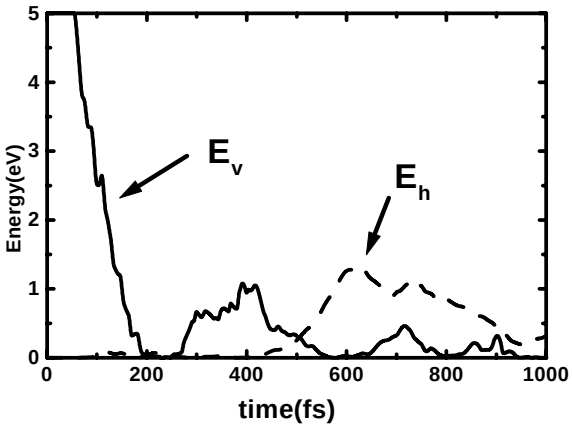

Fig. 3. The same as in Figure 2, but for the Time evolution of the vertical kinetic energy $E_{\rm v}$ (solid line) and the horizontal kinetic energy $E_{\rm h}$ (dashed line) of the C_{20} molecule.

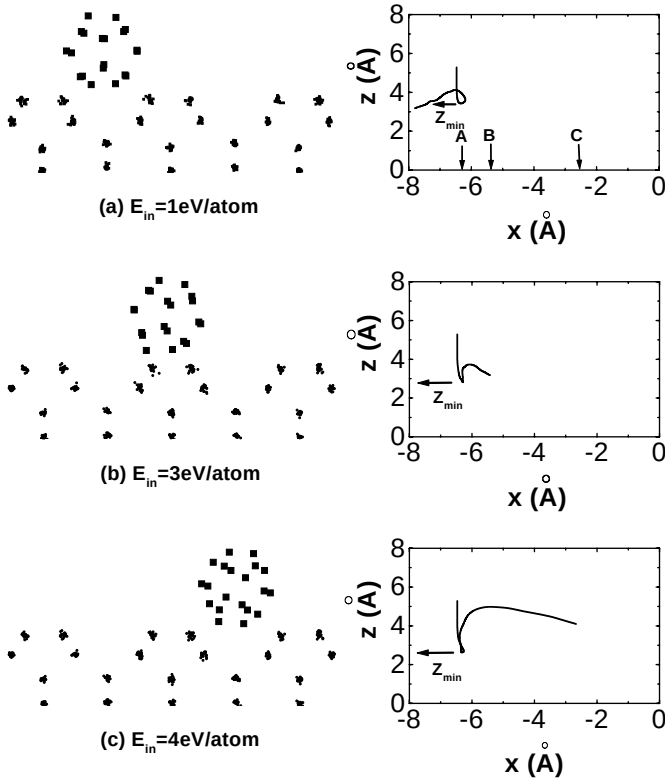

Fig. 4. Snapshots of the final positions ($\sim$ 1 ps) of atoms of C_{20} and silicon surface with different impact energies $E_{\rm in}$. (a) $E_{\rm in} = 1$ eV/atom, (b) $E_{\rm in} = 3$ eV/atom, (c) $E_{\rm in} = 4$ eV/atom. The initial position of the C_{20} molecule is the same as in Figure 2. The solid lines in the right panels shows the trajectories of the mass center of the C_{20} molecule, where the abscissa is along $\langle 110 \rangle$ direction (the dashed line showed in Fig. 1), and the ordinate shows the height above the silicon surface. $Z_{\rm min}$ is the closest distance between the CM of C_{20} and the surface before adsorption. See Figure 1 for the definition of A, B, and C.

When it has enough center-of-mass (CM) kinetic energy it jumps over the dimer and moves to the next trough, and then moves back to the dimer and finally comes to reside on the top of the dimer. At the same time, the bond length of the corresponding dimer is enlarged from 2.37 Å to 2.45 Å to fit the upper C_{20} molecule. This feature is quite similar to the dimer opening effect for the CH_3-diamond interaction [22]. Furthermore, the kinetic properties of the CM energy are presented in Figure 3, which shows that the collision process can be divided into two steps. In the first step ($0 \sim 200$ fs), the C_{20} molecule reaches the closest distance ($Z_{\rm min}$) to the silicon surface with its translational energy transferred into the internal kinetic energy and potential energy of both the C_{20} molecule and the silicon substrate. In the second step, the C_{20} molecule relaxes and gains the kinetic energy again. It first bounces off the surface a little due to the repulse force and gains the vertical kinetic energy ($E_{\rm v}$) again. Then it gets the horizontal kinetic energy ($E_{\rm h}$) due to the anisotropic dimer structures of the silicon surface and moves alone $\langle 110 \rangle$ direction. The maximal value of $E_{\rm h}$ is 1.2 eV. We can see that the lateral motion of the C_{20} molecule is strongly dependent upon the anisotropic molecule-surface interaction. In the following discussions, we study the energy dependence of the lateral motion of C_{20} by varying the incident kinetic energy, $E_{\rm in}$, from 1 eV/atom to 5 eV/atom with increment of 1 eV/atom. The impact points in all these events are selected at position A. The side view of the final adsorption configurations of C_{20} as well as the trajectories of its CM for three typical impact energies are given in Figure 4, where the ordinate is along $\langle 001 \rangle$ direction and the abscissa is $\langle 110 \rangle$ direction. To make the comparison clearer, different values of $Z_{\rm min}$ are presented, which is dependent on the impact energy of C_{20}. In the case of 1 eV/atom, upon arriving on the surface, the C_{20} moves along the $\langle 110 \rangle$ direction to a trough and finally rests at the bottom. In the cases of 2 eV/atom and 3 eV/atom, the behaviors of the C_{20} cluster are quite similar. Therefore only the case of the 3 eV/atom is shown. The C_{20} molecule moves right to the dimer and does not have enough kinetic energy to jump out of the potential well formed by the interaction between the open dimer and the cluster. With an initial energy of 4 eV/atom, it can overcome the potential well of the dimer and at the end rests at the bottom of the trough to the right. While an impact energy of 5 eV/atom, the C_{20} rolls over the dimer to the trough on the right and then rolls back to the dimer as shown in Figure 2. In this case, the C_{20} cluster gets closer to the silicon surface due to its relatively higher initial energy. Therefore, stronger repulsive force are applied to the atoms in the cluster, and further lateral motion of CM is observed. In all these cases, C_{20} is found having little displacement along $\langle \bar{1}10 \rangle$ direction. With much higher energy (10 eV/atom, which is above the cohesive energy), the C_{20} cluster is inlaid in the trough and the damage on the silicon substrate is observed. When the C_{20} impacts at position B (over trough) and C (over dimer), the molecule sticks directly on the surface (in trough or on dimer) with little displacement in both directions. The behavior of the C_{20} molecule is quite similar to that of a C_{60} molecule on the Si (001) surface [23,24]. We will focus our attention

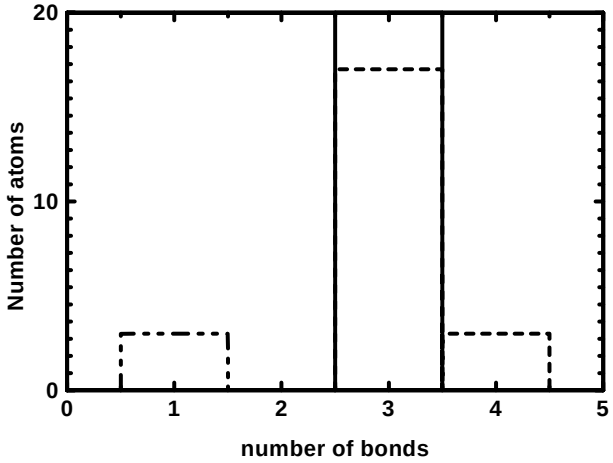

Fig. 5. The distribution of the chemical bonds between the C_{20} and the silicon surface. The solid line represents the case before collision. The dashed line represents the distribution after the collision. The dot-dashed line shows the C–Si bond.

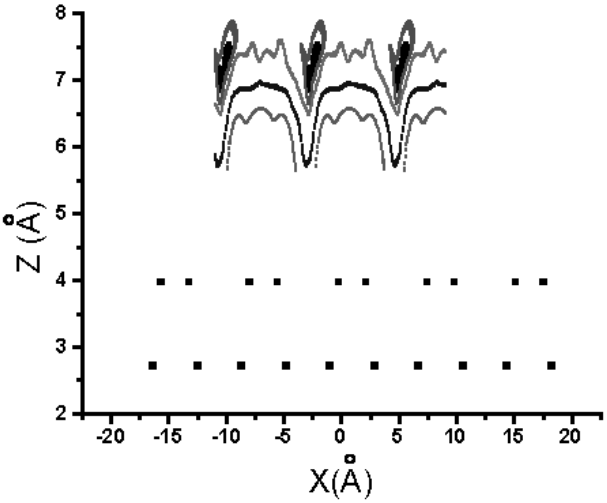

Fig. 6. Potential energy contours as a function of lattice position on the silicon surface. From the bottom to the top, the curves represent different cohesive emerges between a rigid C_{20} cluster and a rigid silicon (001)-(2 × 1) surface, *i.e.*, 100 eV, 20 eV, −0.5 eV, −1.5 eV, −2.5 eV, respectively. The top two layers of silicon atoms are also shown for clarity.

on the low-energy region (1 eV/atom ∼ 5 eV/atom) in the following discussions, since high-energy induced damage is beyond the scope of the present study.

Since there are two energy minimal of the C_{20} on silicon surface, we want to know the chemical bond distributions between C_{20} and silicon. Figure 5 shows the distribution of chemical bonds for the case of the trough-adsorption. To make it clear, we only consider the bonds of the C_{20}. The statistics are carried out within 1 ps after the system reaches a quasi-equilibrium state. The solid line represents the distribution before collision. In the beginning, the C_{20} molecule has 20 carbon atoms, each has 3 bonds with other carbon atoms. The dashed line represents the distribution after the collision. When the C_{20} is adsorbed on the silicon surface at the end of our simulation, three C–Si bonds are formed between the C_{20} and silicon substrate. Similar distribution is got for the case of dimer-adsorption. The binding energy are 20.2 eV (6.7 eV/bond) for trough-adsorption and 21.5 eV (7.13 eV/bond) for dimer-adsorption, respectively. The latter is found to be stronger than that for a linear molecule and other small carbon clusters (C_2, C_3) [14].

To understand the mechanism of the lateral displacement of the C_{20} cluster on the silicon surface, potential energy contours representing the distribution of force field in X-Z plane have been calculated and shown in Figure 6, in which X is alone $\langle 110 \rangle$ direction and Z is normal to the surface. The force field along $\langle \bar{1}10 \rangle$ direction is shown nearly symmetry and not presented here. A relatively simple model, *i.e.*, the interaction between a rigid C_{20} molecule and a rigid silicon substrate is employed. According to this model, the troughs are energy minima of the C_{20}-silicon adsorption. In Figure 6, from the bottom to the top, the curves represent different cohesive energies between a rigid C_{20} cluster and a rigid silicon (001)-(2×1) surface, *i.e.*, 100 eV, 20 eV, −0.5 eV, −1.5 eV, −2.5 eV, respectively. According to this picture, when the C_{20} molecule impacts on B site (dimer) or C site (trough), it tends to stay in the potential well and therefore absorption configuration forms. When the C_{20} molecule impacts on the A site, the lateral gradient of the force field is strongly dependent on the closest distance between the CM of C_{20} and the surface ($Z_{\min}$), which is related to the impact energy of C_{20}. Therefore impact energy is an important factor that can influence the collective motion of the C_{20} molecule on silicon surface. With low impact energy (say, 1 eV/atom), the C_{20} molecule directly moves to the trough (potential well) due to the the gradient of the force field. With relatively higher kinetic energy, the C_{20} molecule can penetrate into laterally adjacent force field. Therefore great changes of the motion of the C_{20} molecule with different impact energy have been found. Also, due to the stronger repulse force between the C_{20} molecule with higher kinetic energy and the silicon surface, the C_{20} molecule can rebound off the impact site and gains enough kinetic energy to move on the silicon surface and overcome the surface potential barriers to a potential minimal and forms bonds with the surface atoms at the end. Unfortunately, this simple model cannot represent the opening of dimer. Therefore it can not exactly explain the dimer-stick of C_{20} molecule. However it exhibits a relatively clear picture of the movement of the C_{20} on silicon surface.

4 Conclusions

The microscopic process of the interaction of the C_{20} and a reconstructed silicon substrate is unveiled by MD simulations. The C_{20} cluster can move as a rigid sphere due to the anisotropic force field between the dimer-row structure of the silicon surface. Different impact energy leads to different closest interaction distance between the C_{20} molecule

and silicon surface, which generates different distribution of force field. Changes in the force field leads to the different kinetic behavior of the C_{20} molecule along the $\langle 110 \rangle$ direction. Little movement of the C_{20} cluster in the $\langle \bar{1}10 \rangle$ direction is found due to the balance of forces applied to the C_{20} cluster in this direction. Finally, the C_{20} cluster comes to rest on the surface when its kinetic energy is consumed. In the trough or on the top of a dimer are the two energy-favored adsorption sites of the C_{20} molecule on a dimerized silicon surface. The formation of C–Si bonds is an indication that strong bindings between the C_{20} and the silicon substrate exist. These results are consistent with experimental findings of a C_{60} fullerene adsorbed on a reconstructed silicon (001) surface. Simulation of interactions between several C_{20} clusters and silicon surface are being carried out. Also, the initial rotation of C_{20} has not been taken into account in the present study, and we plan to address this problem in the near future.

This work is supported partly by the National Natural Science Foundation of China under Grant No. 19875011.

References

1. C. Yeretzian, K. Hansen, R.D. Beck, R.L. Whetten, J. Chem. Phys. **98**, 7480 (1993).
2. H.G. Busmann, Th. Lill, I.V. Hertel, Chem. Phys. Lett. **187**, 459 (1991).
3. R.D. Beck, P.St. John, M.M. Alvarez, F. Diederich, R.L. Whetten, J. Phys. Chem. **95**, 8402 (1991).
4. R.C. Mowrey, D.W. Brenner, B.I. Dunlap, J.W. Mintmire, C.T. White, J. Phys. Chem. **95**, 7138 (1991).
5. P. Blaudeck, Th. Frauenheim, H.-G. Busmann, T. Lill, Phys. Rev. B **49**, 11409 (1994).
6. Z.Y. Man, Z.Y. Pan, H.K. Ho, Phys. Lett. A **208**, 53 (1995).
7. R. Smith, K. Beardmore, Thin Solid Films **272**, 255 (1996).
8. A. Perez *et al.*, J. Phys. D Appl. Phys. **30**, 709 (1997).
9. P.R. Taylor, E. Bylaska, J.H. Weare, R. Kawai, Chem. Phys. Lett. **235**, 558 (1995).
10. V. Paillard *et al.*, Phys. Rev. B **49**, 11433 (1994).
11. J. Tersoff, Phys. Rev. B **39**, 5566 (1989).
12. W. Eckstein, *Computer Simulations of Ion-Solid Interactions* (Springer, Berlin, 1991).
13. T. Halicioglu, Thin Solid Films **260**, 200 (1995).
14. T. Halicioglu, Thin Solid Films **249**, 78 (1994).
15. T. Halicioglu, Thin Solid Films **286**, 184 (1996).
16. Zhenyong Man, Zhengying Pan, Jun Xie, Yukun Ho, Nucl. Instr. Meth. Phys. Res. B **135**, 342 (1998).
17. V. Parasuk, J. Almlöf, Chem. Phys. Lett. **184**, 187 (1991).
18. R. Smith, D.E. Harrison, B.J. Garrison, Phys. Rev. B **40**, 93 (1989).
19. F.Z. Cui, H.D. Li, X.Y. Huang, Phys. Rev. B **49**, 9962 (1994).
20. D. Brown, J.H.R. Clarke, Molec. Phys. **51**, 1243 (1984).
21. L. Verlet, Phys. Rev. A **159**, 98 (1967).
22. B.J. Garrison, E.J. Dawnkaski, D. Srivastava, D.W. Brenner, Science **255**, 835 (1992).
23. D. Klyachko, D.M. Chen, Phys. Rev. Lett. **75**, 3693 (1995).
24. T. Hashizume *et al.*, Jpn J. Appl. Phys. **31**, L880 (1992).